Prospects for observing and localizing Gravitational-Wave transients with Advanced LIGO, Advanced Virgo and KAGRA

ALICE GABRIELLI

- GW Detectors and main results of the first two runs
- Sensitivity and Range for the different observing runs
- Searches for gravitational-wave transients
- Detection and False Alarm Rates
- Localization of the source
- Observing scenarios

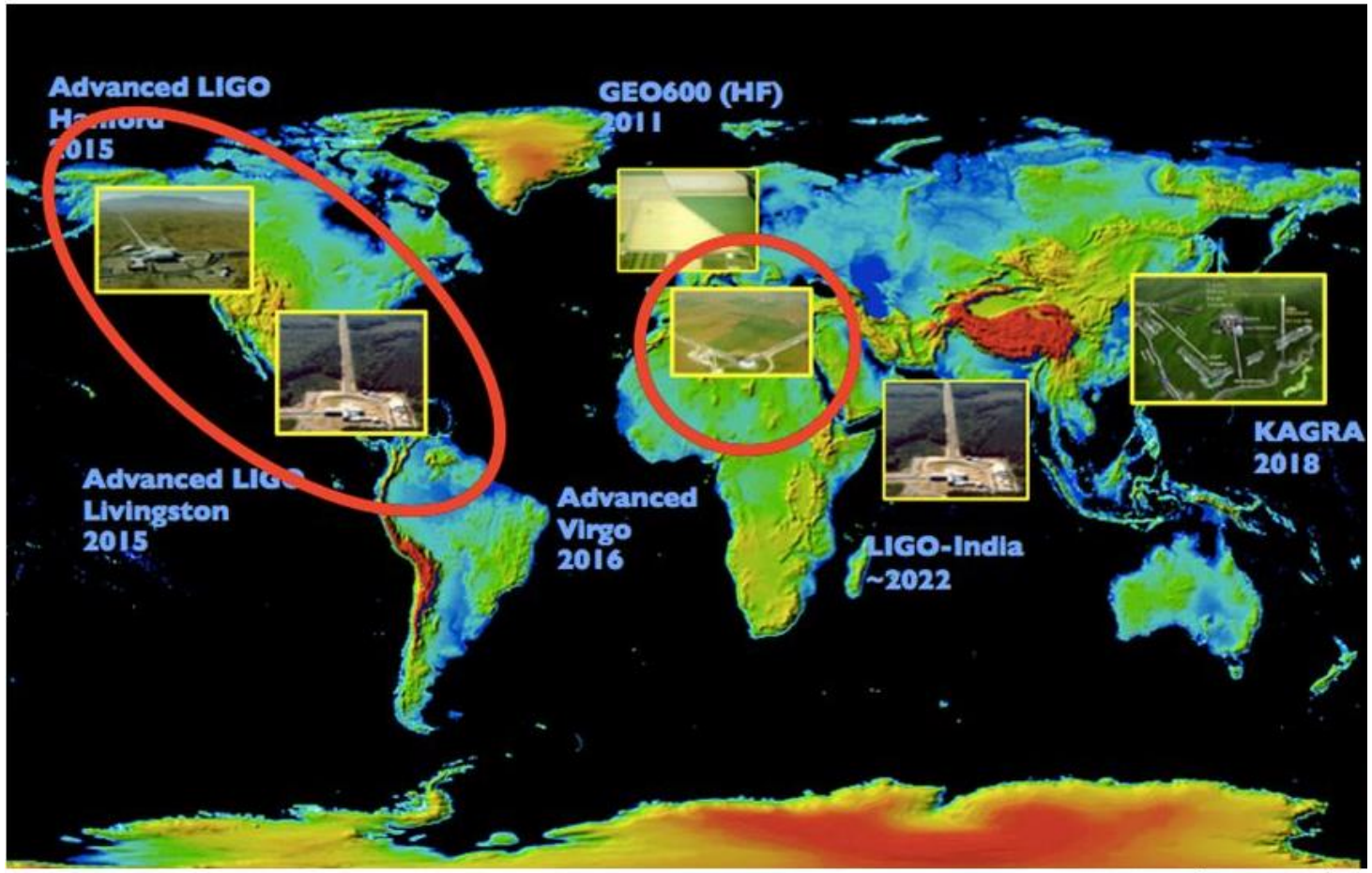

Hanford (Washington) Livingstone (Louisiana) Virgo (Cascina)

Main GW detectors that are used and will be used in LIGO-Virgo collaboration

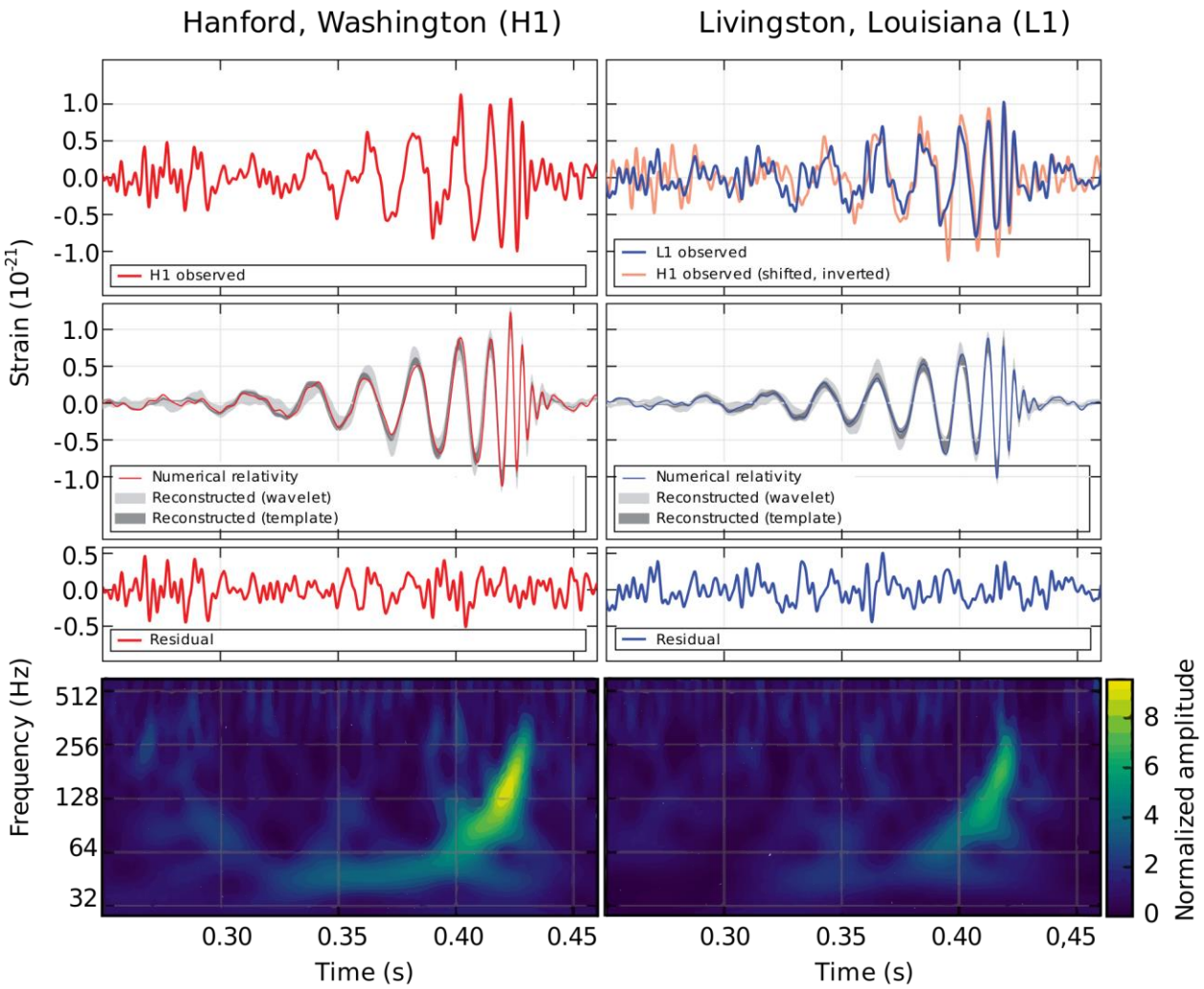

First observation of GW: GW150914

September 2015

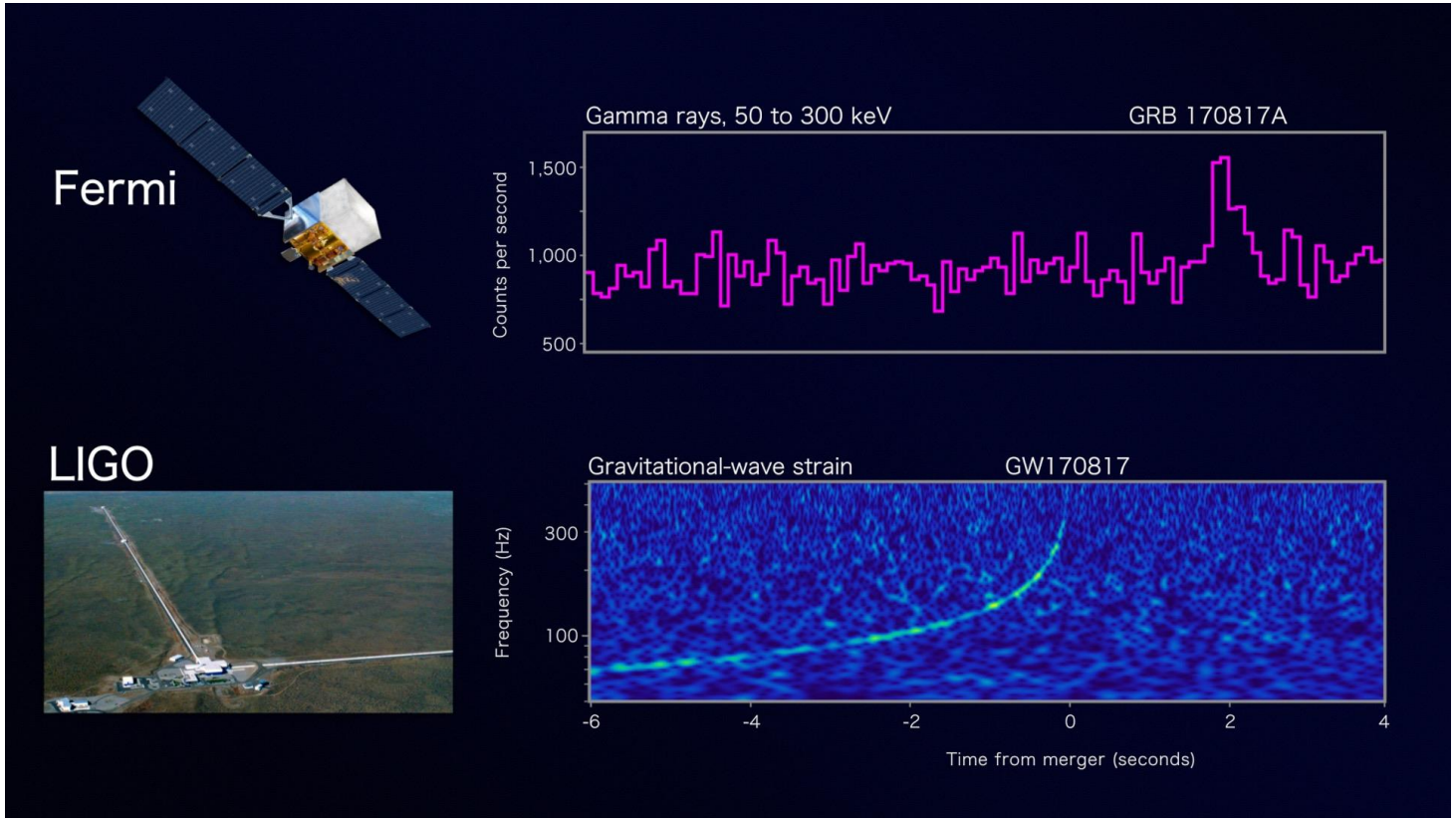

First confirmed multi-messenger counterpart to a GW observation

August 2017

We divide the development of the GW observatories into three components:

- Construction includes the **installation and testing** of the detectors (no astrophysically results).
- Commissioning **improves the detectors' performance** with the goal of reaching the design sensitivity (these are not intended to produce astrophysical results, but that does not preclude the possibility of this happening)
- **Observing runs** begin when the detectors have reached (and can stably maintain) a significantly improved sensitivity compared with previous operation. (astrophysically results, direct detections from some GW sources and upper limits on the rates or energetics of others.)

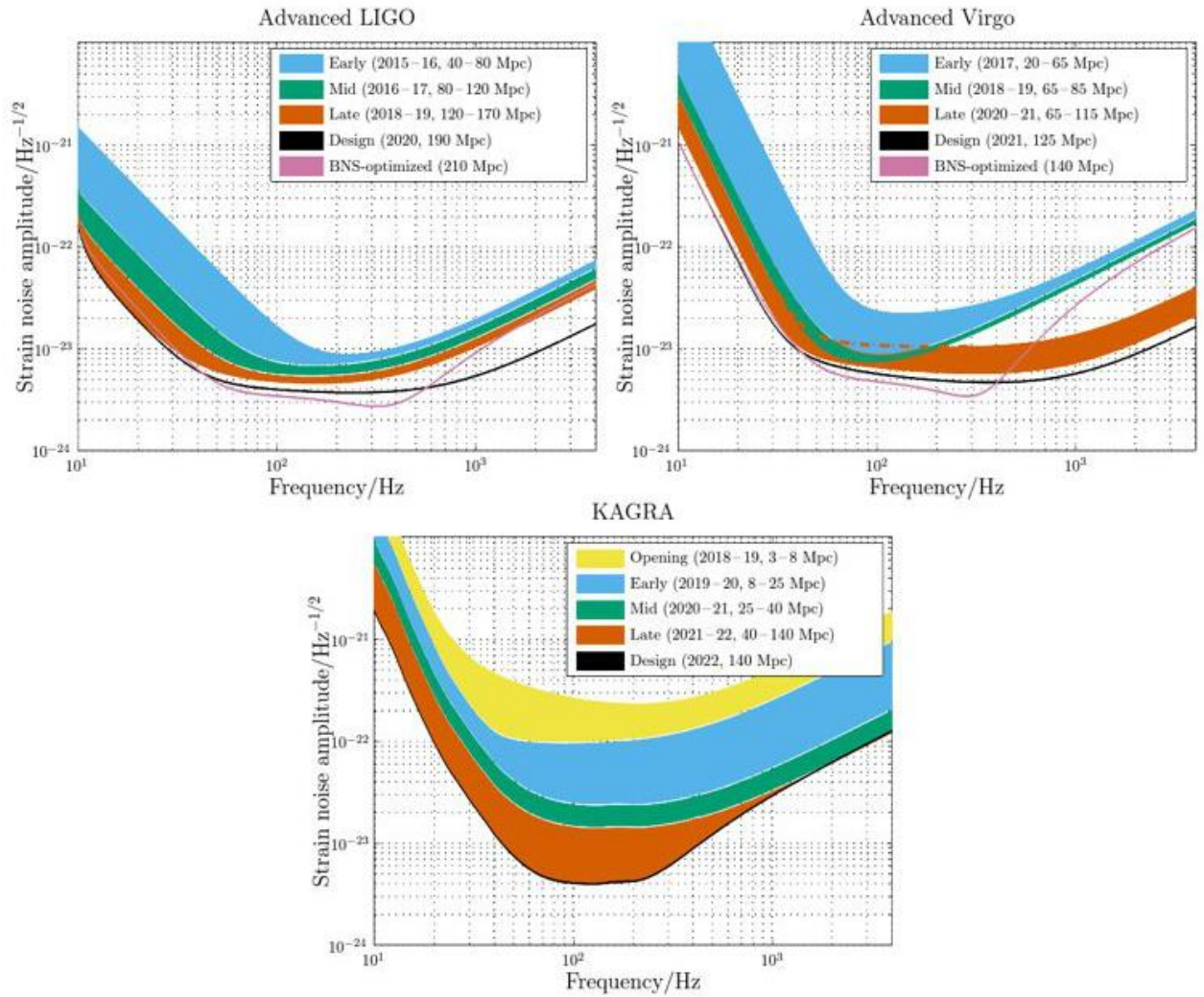

The strain sensitivity evolution for aLIGO, AdV and KAGRA as a function of BNS range

Sensitivity and Range

As a standard figure of merit for detector sensitivity, we use the range, the volume- and orientation-averaged distance at which a compact binary coalescence consisting of a particular mass gives a matched filter signal-to-noise ratio (SNR) of 8 in a single detector.

We define V_z as the orientation-averaged spacetime volume surveyed per unit detector time.

For a population with a constant comoving source-frame rate density, V_z multiplied by the rate density gives the detection rate of those sources by the particular detector.

We define the range R as the distance for which

$$\frac{4}{3}\pi R^3 = V_z$$

Table 1 Plausible target detector sensitivities. The different phases match those in Fig. 1. We quote the range, the average distance to which a signal could be detected, for a $1.4M_{\odot}$+$1.4M_{\odot}$ binary neutron star (BNS) system and a $30M_{\odot}$+$30M_{\odot}$ binary black hole (BBH) system.

	LIGO		Virgo		KAGRA	
	BNS range/Mpc	BBH range/Mpc	BNS range/Mpc	BBH range/Mpc	BNS range/Mpc	BBH range/Mpc
Early	40 – 80	415 – 775	20 – 65	220 – 615	8 – 25	80 – 250
Mid	80 – 120	775 – 1110	65 – 85	615 – 790	25 – 40	250 – 405
Late	120 – 170	1110 – 1490	65 – 115	610 – 1030	40 – 140	405 – 1270
Design	190	1640	125	1130	140	1270

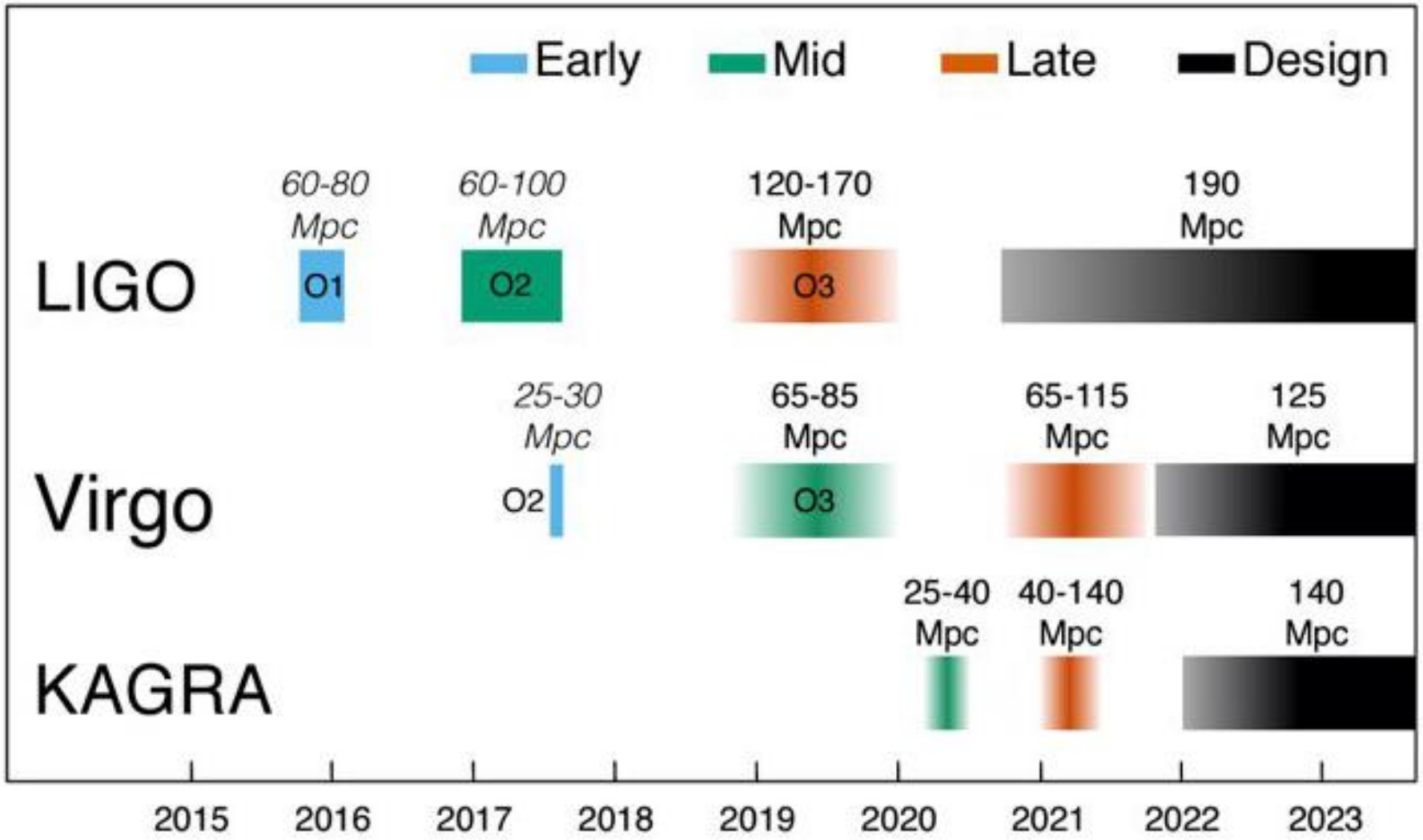

Subsequent observing runs have increasing duration and sensitivity.

Searches for gravitational-wave transients

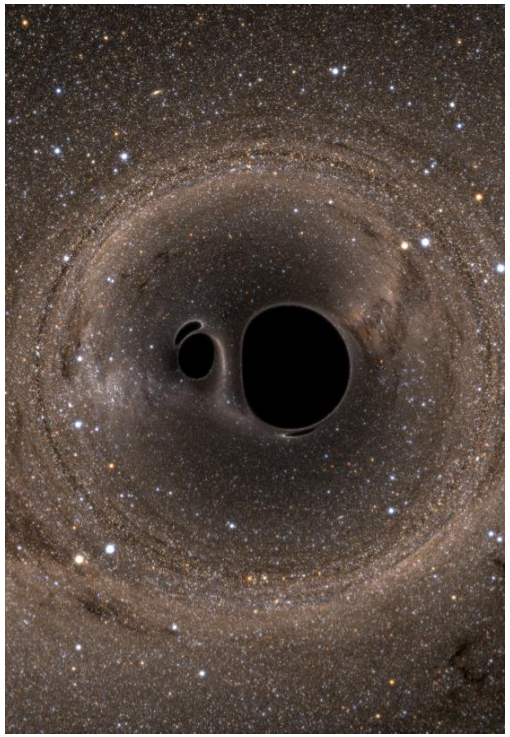

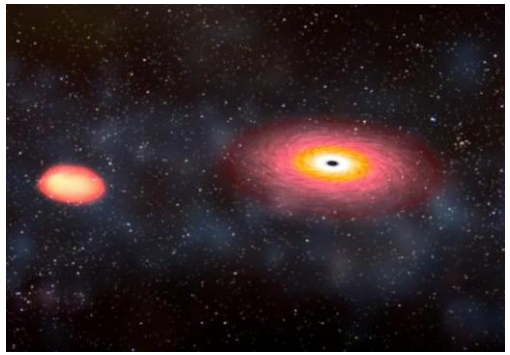

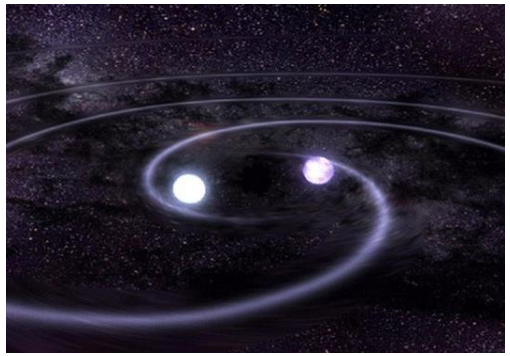

Focus on signals from compact binary coalescences (CBCs) and on generic transient or burst signals. CBCs include BNS, neutron star–black hole (NS–BH) and BBH systems.

The gravitational waveform from the **inspiral phase of a BNS coalescence** is well modeled and **matched filtering** can be used to search for signals. For systems containing black holes, or in which the component spin is significant, uncertainties in the waveform model can reduce the sensitivity of the search.

Searches for **bursts** make few assumptions on the **signal morphology**, using time–frequency decompositions to identify statistically significant excess-power transients in the data. Burst searches generally perform best for short-duration signals (. 1 s), although search development remains an area of active research.

Prior to O1, 74 teams signed MOUs to participate in the electromagnetic follow-up program, and for the first event candidate later confirmed as GW150914, 63 were operational and covered the full electromagnetic spectrum. For **the first observations** with the advanced detectors, thorough checks were performed before alerts were released, resulting in **latencies much greater than 1 h**. We expect this latency to be improved in the future as we gain experience with the instruments, and aim for automatic alerts being sent out with only a few minutes latency; continued checks may lead to retractions of some of these low-latency alerts. In the case of GW150914, 25 teams responded to the GW alert and operated ground- and space-based instruments spanning 19 orders of magnitude in electromagnetic wavelength.

No significant electromagnetic counterpart and no afterglow emission was found in optical, ultraviolet, X-rays, or GeV gamma rays. The weak transient found in Fermi-GBM data 0.4 s after GW150914 was not confirmed by other instruments like INTEGRAL SPI-ACS, AGILE or any other experiments of the InterPlanetary Network.

GW170817 was **the first GWtransient** for which a firm electromagnetic counterpart was discovered. On 2017 August 17 12:41:06 UTC, Fermi-GBM triggered on a short GRB, GRB170817A , and a GCN was sent after 14 s. About 6 min later, a GW trigger was identified; the signal was consistent with a BNS coalescence occurring $\sim$1.7 s before GRB170817A

Increased detection confidence, improved sky localization, and identification of host galaxy and redshift are just some of the benefits of joint GW–electromagnetic observations.

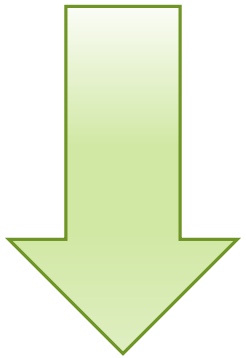

We focus on two points of particular relevance for follow-up of GW events: the source localization afforded by a GW network as well as the relationship between signal significance, or false alarm rate (FAR), and source localization.

Detection and False Alarm Rates.

- Detection pipelines search the data looking for signal-like features.

Candidate triggers flagged by a pipeline are assigned a detection statistic to quantify how signallike they are.

For CBC searches, this involves matching a bank of waveform templates to the data.

For burst searches, requirements on waveform morphology are relaxed, but coherence of the signal in multiple detectors is required.

- The FAR is then the total number of expected candidates from noise divided by the live time of the experiment,T.

The detection statistic is used to rank candidates.

We assess significance by comparing results with those from an estimated background distribution of noise triggers.

It is difficult to theoretically model the behaviour of non-Gaussian noise, and therefore the distribution must be estimated from the data.

From the background noise distribution, we can map a value of the detection statistic to a FAR, the expected rate of triggers with detection statistics equal to or greater than that value, assuming that the data contain no signals.

While each pipeline has its own detection statistic, they all compute a FAR, making it easy to compare results. The FAR, combined with the observation time, may then be used to calculate a p value, the probability of there being at least one noise trigger with a FAR this small or smaller in the observed time.

As the FAR or p value of a trigger decreases, it becomes more significant, and more likely to be a genuine astrophysical signal.

Search pipelines are run both online, analysing data as soon as they are available in order to provide low-latency alerts of interesting triggers, and offline, taking advantage of improved calibration of the data and additional information regarding data quality.

Localization

Following the detection of a GW transient posterior probability distributions for the position are constructed following a Bayesian framework, with information for the sky localization coming from the time of arrival, plus the phase and amplitude of the GW.

An intuitive understanding of localization can be gained by considering triangulation using the observed time delays between sites . The effective single-site timing accuracy is approximately

$$\sigma_t = \frac{1}{2\pi\rho\sigma_f}$$

where ρ is the SNR in the given detector and σ_f is the effective bandwidth of the signal in the detector, typically of order 100 Hz.

The timing-triangulation approach underestimates how well a source can be localized, since it does not include all the relevant information. Its predictions can be improved by introducing the requirement of phase and amplitude consistency between detectors.

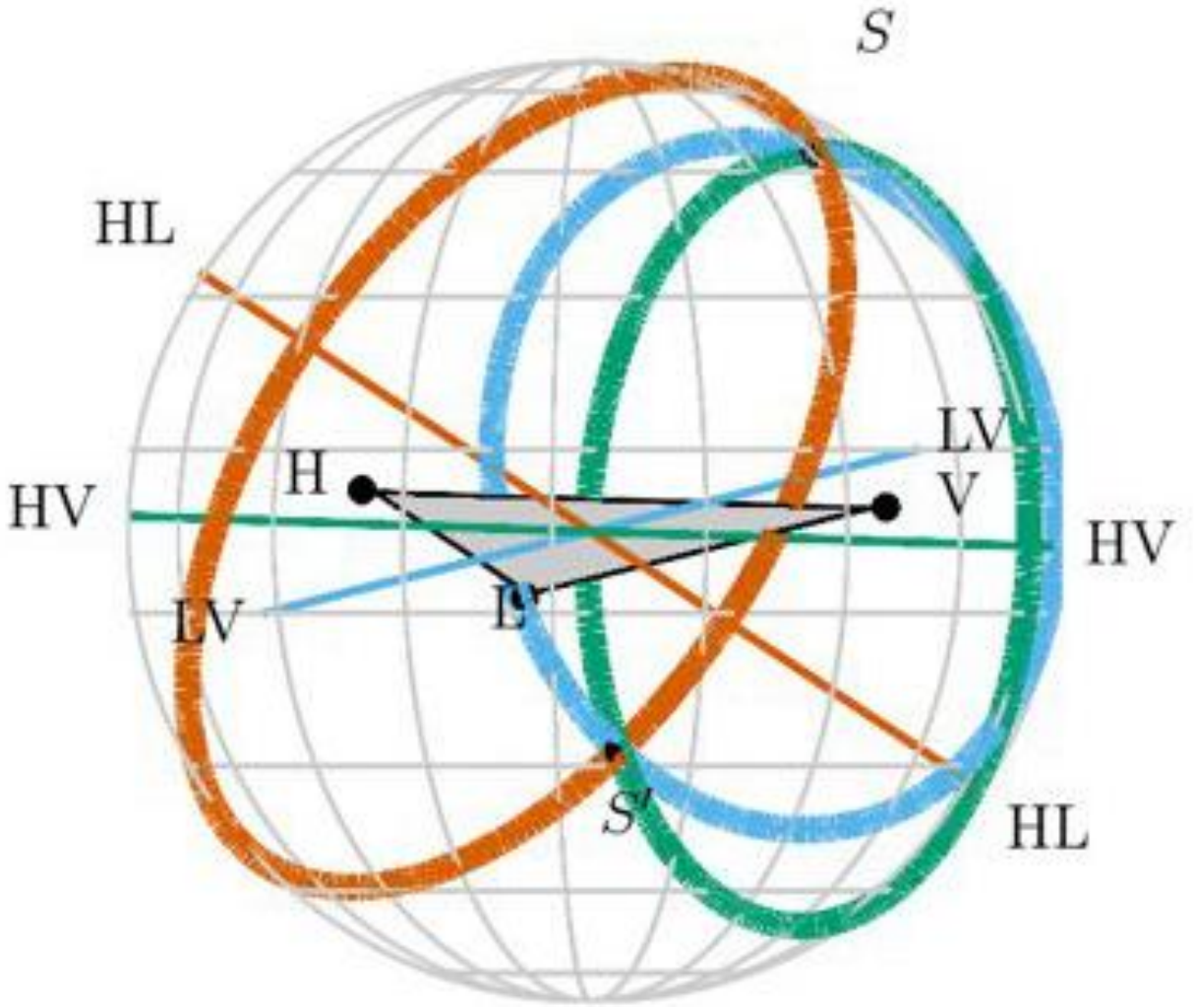

Source localization by timing triangularization for the aLIGO-AdVirgo network

Low-latency BAYESTAR code

High-latency LALInference code

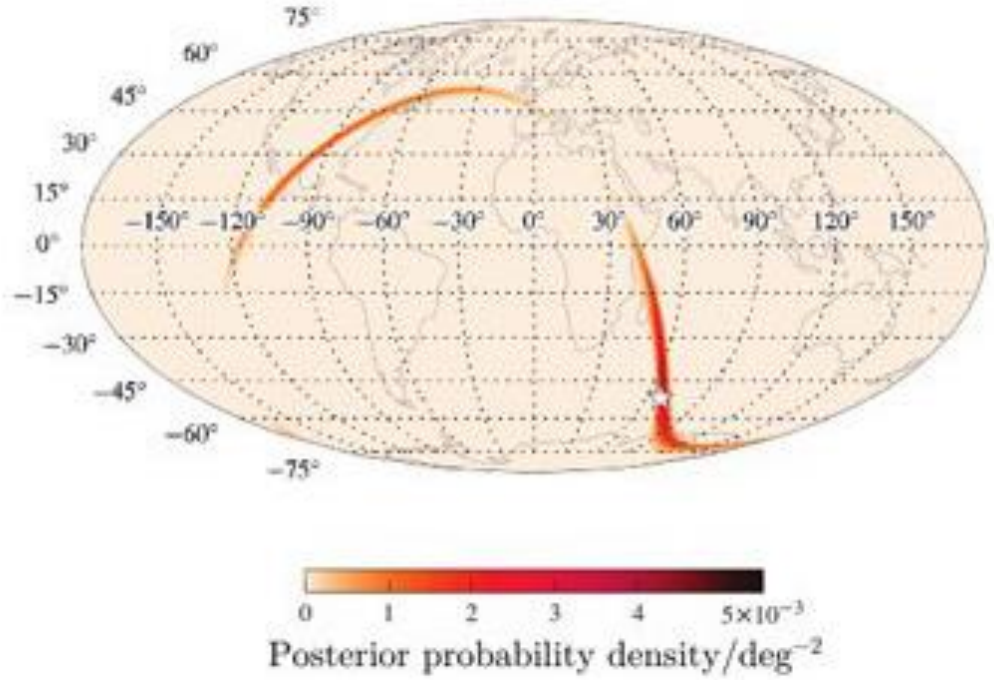

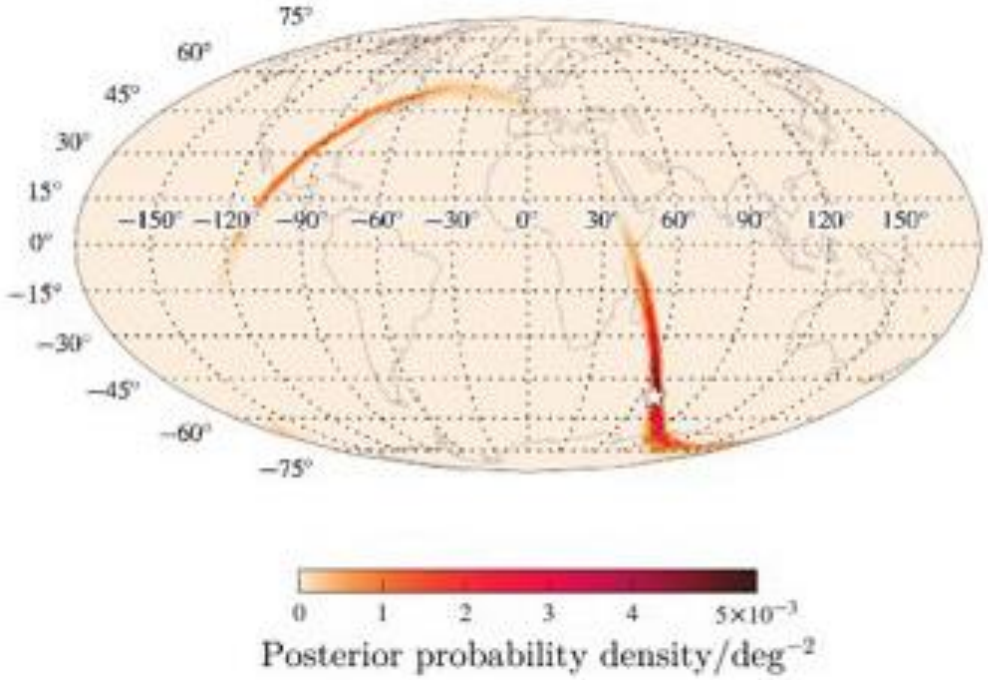

Posterior probability density for sky location for an example simulated binary neutron star coalescence observed with a two-detector network.

For signals just above the detection threshold, this typically yields regions with areas of several tens to hundreds of square degrees.

If there is significant difference in sensitivity between detectors, the source is less well localized and we may be left with the majority of the annulus on the sky determined by the two most sensitive detectors. With four or more detectors, timing information alone is sufficient to localize to a single sky region, and the additional baselines help to limit the region to under 10 deg2 for some signals.

From the effective single-site timing accuracy, it follows that the linear size of the localization ellipse scales inversely with the SNR of the signal and the frequency bandwidth of the signal in the detector

Higher mass CBC systems merge at lower frequencies and so have a smaller effective bandwidth. For burst transients, the bandwidth sf depends on the specific signal.

In addition to localizing sources on the sky, for CBC signals it is possible to provide distance estimates, since the waveform amplitude is inversely proportional to the luminosity distance. Uncertainty in distance measurement is dominated by the degeneracy with the binary's inclination, which also determines the signal amplitude

Observing scenarios

In this section we estimate the sensitivity, possible number of detections, and localization capability for each of the observing runs. In the following, we estimate the expected number of BNS coalescence detections using the inferred 90% credible range for the BNS source rate density, 320 – 4740 $Gpc^{-3}\ yr^{-1}$.

Given the detectors' noise spectral densities, the ρ_c detection threshold can be converted into the (source sky-location and orientation averaged) BNS sensitive detection range R_{BNS}.

The BNS source rate density can be converted into an estimate of the number of expected detected events; this estimate carries the large error on the source rate density.

We assume a nominal ρ_c threshold of 12, at which the expected FAR is $10^{-2}\ yr^{-1}$.

Detector		Hanford	Livingston
Operating mode %	Observing	64.6	57.4
	Locking	17.9	16.1
	Environmental	9.7	19.8
	Maintenance	4.4	4.9
	Commissioning	2.9	1.6
	Planned engineering	0.1	0.0
	Other	0.4	0.4

Percentage of time during the first observing run that the LIGO detectors spent in different operating modes

2015 – 2016 run (O1): aLIGO

This was the first advanced-detector observing run, lasting four months.

The O1 BNS search volume was $\sim 2 \times 10^5\ Mpc^3 yr$, and the dominant source of uncertainty on this value is the calibration of the detectors.

We would therefore expect 0.05 – 1 BNS detections. No BNS detections were made, consistent with these expectations

The median 90% credible region for is 460 – 530 deg^2; the searched area is smaller than 20 deg^2 for 14 – 17% of events and smaller than 5 deg^2 in 4 – 6%

2016 – 2017 run (O2): aLIGO joined by AdV

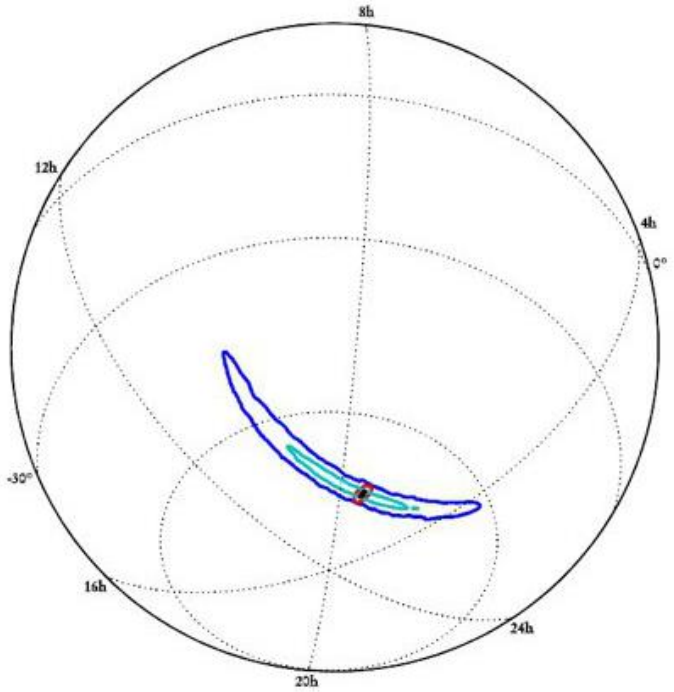

This was an approximately nine-month run with three detectors for the second part of the run. With a BNS range of 80 – 120 Mpc, and a burst range of 60 – 75 Mpc:the achieved BNS range is towards the lower part of this band, around 60 – 100 Mpc.

On 1 August 2017, AdV joined O2 with a BNS range of 25 – 30 Mpc. The potential improvement in sky localization from the addition of a third detector is illustrated in Figure.

The searched area is smaller than 20 deg^2 for 33 – 41% of events and smaller than 5 deg^2 for 16 – 21%

2018 – 2019 run (O3): aLIGO 120 – 170 Mpc, AdV 65 – 85 Mpc

This is envisioned to be a year long run with three detectors. With BNS ranges of 120 – 170 Mpc and 65 – 85 Mpc, and burst ranges of 75 – 90 Mpc and 40 – 50 Mpc.

This gives an expected update 1 – 50 BNS detections.

The median 90% credible region is 120 – 180 deg^2, and 12 – 21% of events are expected to have 90% credible region smaller than 20 deg^2.

2020+ runs: aLIGO 190 Mpc, AdV 65 – 125 Mpc

The aLIGO detectors are expected to have a sensitivity curve similar to the design curve.

The fraction of signals localized to areas of a few square degrees is increased compared to previous runs.

This is due to the much larger detector bandwidths, particularly for AdV, as well as the increased sensitivity of the network;

2024+ runs: aLIGO (including LIGO-India) 190 Mpc, AdV 125 Mpc, KAGRA 140 Mpc

The five-site network incorporating LIGO-India at design sensitivity would have both improved sensitivity and better localization capabilities. The per-year BNS search volume increases giving an expected 11 – 180 BNS detections annually. The addition of more detector sites leads to good source localization over the whole sky.

The median 90% credible region is 9 – 12 deg^2, 65 – 73% of events are expected to have 90% credible region smaller than 20 deg^2, and the searched area is less than 20 deg^2 for 87 – 90% .

Epoch			2015–2016	2016–2017	2018–2019	2020+	2024+
Planned run duration			4 months	9 months	12 months	(per year)	(per year)
Expected burst range/Mpc		LIGO	40–60	60–75	75–90	105	105
		Virgo	—	20–40	40–50	40–70	80
		KAGRA	—	—	—	—	100
Expected BNS range/Mpc		LIGO	40–80	80–120	120–170	190	190
		Virgo	—	20–65	65–85	65–115	125
		KAGRA	—	—	—	—	140
Achieved BNS range/Mpc		LIGO	60–80	60–100	—	—	—
		Virgo	—	25–30	—	—	—
		KAGRA	—	—	—	—	—
Estimated BNS detections			0.05–1	0.2–4.5	1–50	4–80	11–180
Actual BNS detections			0	1	—	—	—
90% CR	% within	5 deg^2	< 1	1–5	1–4	3–7	23–30
		20 deg^2	< 1	7–14	12–21	14–22	65–73
	Median/deg^2		460–530	230–320	120–180	110–180	9–12
Searched area	% within	5 deg^2	4–6	15–21	20–26	23–29	62–67
		20 deg^2	14–17	33–41	42–50	44–52	87–90

Summary of a plausible observing schedule,expected sensitivities, and source localization with aLIGO, AdVirgo and KAGRA detectors network